Functional extensions of Dip Pen Nanolithography^{TM}: active probes and microfluidic ink delivery

2006 Smart Mater. Struct. 15 S124

(http://iopscience.iop.org/0964-1726/15/1/020)

INSTITUTE OF PHYSICS PUBLISHING SMART MATERIALS AND STRUCTURES
Smart Mater. Struct. **15** (2006) S124–S130 doi:10.1088/0964-1726/15/1/020

Functional extensions of Dip Pen Nanolithography™: active probes and microfluidic ink delivery

Bjoern Rosner[1], Terrisa Duenas[2], Debjyoti Banerjee[2], Roger Shile[2], Nabil Amro[1] and Jeff Rendlen[1]

[1] NanoInk Incorporated, Corporate Office, 1335 Randolph Street, Chicago, IL 60607-1523, USA
[2] NanoInk Incorporated, MEMS Fabrication, 215 East Hacienda Avenue, Campbell, CA 95008-6616, USA

Received 9 May 2005
Published 13 December 2005
Online at stacks.iop.org/SMS/15/S124

Abstract
Dip Pen Nanolithography (DPN™) is an important technique for nanotechnology and a fundamental new tool for studying the consequences of miniaturization. In this scanning probe technique a sharp tip is coated with a functional molecule (the 'ink') then brought into contact with a surface where it deposits ink via a water meniscus. The DPN process is a direct-write pattern transfer technique with nanometer resolution and is inherently general with respect to usable inks and substrates, including biomolecules such as proteins and oligonucleotides. We present functional extensions of the basic DPN process by showing multiple active probes along with the ability to load different inks onto probe tips. We present the fabrication process and characterization of thermomechanically actuated probes that use the bimorph effect to induce deflection of individual cantilevers as well as the integration of these probes with control electronics and an interface module. As an additional improvement to DPN functionality, we developed the capability to write with different inks on the probe array, permitting the fabrication of multicomponent nanodevices in one writing session. For this purpose, we fabricate passive microfluidic devices and present the microfluidic behavior and ink loading performance of these components.

(Some figures in this article are in colour only in the electronic version)

1. Introduction

The invention of scanning tunneling microscopy in the early 1980s by Binnig and Rohrer [1] and the subsequent development of other scanning probe microscopy (SPM) techniques, most notably atomic force microscopy (AFM) [2], made much of nanotechnology accessible. SPM includes the direct observation of structures at atomic and molecular dimensions; the ability to measure a myriad of physical properties at the smallest scale—often in parallel; and finally the fabrication of structures using various scanning probe microscopy techniques—collectively known as scanning probe lithography. These surface modification techniques can be further divided into the categories found in their molecular-scale chemical synthesis counterparts—that is, additive lithography, subtractive lithography, and substitutive lithography [3]. Dip Pen Nanolithography (DPN) [4] is the most prevalent form of additive lithography and is a commercialized process [5, 6]. As such, aspects of the process such as reliability, repeatability, optimization, and throughput are of concern as well as ease of use through software, hardware integration and automation. Moreover, because it is a successful method of organizing material on the nanometer scale to manipulate structures into nanodevices [7, 8], applied DPN is also a veritable example of nanotechnology.

The DPN process uses a chemically coated scanning probe tip (the 'pen') to directly deposit a material ('ink') with nanometer precision onto a substrate [4, 9]. Under ambient

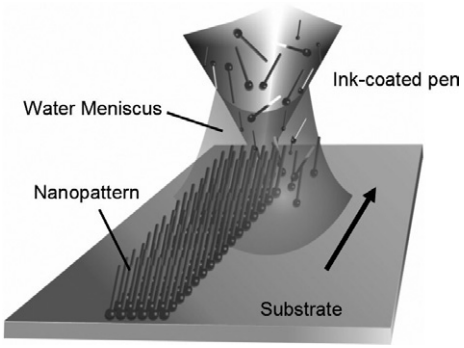

Figure 1. Schematic diagram of Dip Pen Nanolithography (DPN).

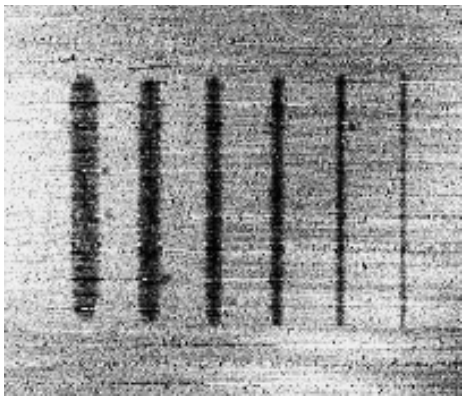

Figure 2. DPN method-generated lines, using 16-mercaptohexadecanoic acid (MHA) as ink on gold. The right-most line is just 26 nm wide.

conditions the DPN process (figures 1 and 2) can deposit a variety of organic and inorganic molecules onto a variety of substrate types [10]. Lines and dots of 15 nm diameter have been demonstrated [11] using 16-mercaptohexadecanoic acid (MHA) on gold. When using oligomer- or protein-based inks, the DPN method can produce nanoscale spotted features which are much smaller than conventional bio-arrays [12, 13]. For example, Mirkin and co-workers [14] used DPN to spot protein nanoarrays using both lysozyme and immunoglobulin G (IgG). The arrays featured structures as small as 100 nm in diameter and were shown to exhibit an almost complete absence of non-specific binding of proteins to passivated areas of the structure. Additional applications of DPN include but are not limited to using DPN patterns as etch resist [15], patterning with magnetic particles [16] and the creation of templates for subsequent particle attachment [17].

2. Microfluidic ink delivery

2.1. Motivation

In the most basic DPN process one pen is submerged and then removed from the ink. In many cases excess ink is removed with a high-pressure blast of air or gas. While this technique can produce good results in skilled hands, it is advantageous to have a more reproducible approach to inking the pen. To improve inking reliability as well as writing reproducibility, we chose to produce microfabricated devices (inkwells) that carry ink and can be brought in contact with the pen to transfer ink onto the pen, an idea inspired by early work by Chang Liu at the University of Illinois at Urbana-Champaign (UIUC). It is of advantage to write with multiple probes simultaneously not only to increase patterning speed and increase area coverage, but also because it allows writing with multiple inks in the same session. Parallel writing via DPN using a one-dimensional array of passive probes was recently reported by Liu and Mirkin [11, 18–20]. The aforementioned inkwells have the same pitch as existing multi-pen arrays (so that many parallel pens can be inked) and consist of multiple ink reservoirs and distribution channels so that adjacent pens can be supplied with different inks without cross-contamination. One additional important use for microfluidic ink delivery is to *NOT* supply ink to specified probes while adjacent probes receive ink. This appears particularly helpful when considering that in basic DPN operation, the inked probe is also used for inspection of the written pattern. While it is commonly assumed that ink transfer is negligible at very high probe scan speed, it can be very advantageous to use an adjacent, non-inked probe for pattern inspection. This allows for slower scan speed with possibly better image quality and less contamination onto the finished pattern.

2.2. Design

The inkwells were designed to deliver at least four different aqueous inks (for example for genomic applications) into an appropriately spaced inkwell array. Fluid actuation occurs by open channel meniscus driven flow (wicking) in micro-channels, which distribute liquid from reservoirs into an array of terminal inkwells connected by tributaries.

To understand the ink-delivery and design channels with useful dimensions, it is necessary to calculate the filling times of microchannels of different sizes, among other considerations [21]. The flow rates in the micro-channels were calculated from a balance of the capillary and viscous forces (neglecting inertial forces), resulting in the following expression [21]:

$$\left[\frac{\sigma \cos\theta / D_{\mathrm{h}}}{4\mu}\right]\tau = \frac{L_2^2 - L_1^2}{D_{\mathrm{h}}^2} \qquad (1)$$

where τ is the filling time, σ the coefficient of surface tension, θ the contact angle, D_{h} the hydraulic diameter of the channel, L the length of the channel and μ the kinematic viscosity of the working liquid. Calculations based on equation (1) show that for the same length the wider channels (larger D_{h}) fill up faster than the narrow channels (see figure 3). This is due to capillary forces ($\sim 1/D_{\mathrm{h}}$) being retarded by an even larger pressure drop ($\sim D_{\mathrm{h}}^2$) in narrow microchannels.

The final design thus consists of relatively wide main channels (20–40 μm) that feed narrower channels (tributaries) of 5 μm width that terminate in 18–20 μm sized microwells (see figure 4). These microwells host the probe tip during inking. Conveniently, this design allows the microwells to stay completely filled while the reservoirs are depleted due to evaporation.

In one of the final designs, two similar devices (seen in figure 4) are grouped on a die. Each contains four ink

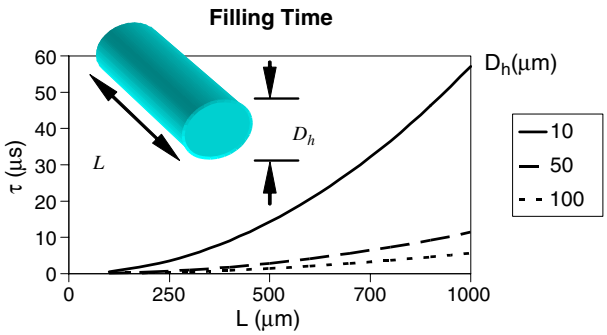

Figure 3. Filling time (τ) in microseconds for capillary pumped flow of water in microchannels of different length (L) and hydraulic diameter (D_h) using equation (1).

reservoirs, sized 1 mm in diameter. Between reservoirs and microwells, air bubble traps are included that increase ink delivery reliability. Alignment marks near the microwells help in orienting the pens in the correct orientation and location.

2.3. Fabrication

For the small volumes used in this application, evaporative losses are not negligible. Deep channels and reservoirs help to keep more liquid in and thus retard the loss of liquid in the microwells. Different wet and dry etching methods were investigated to fabricate features with high aspect ratio (10:1). Deep reactive ion etching (DRIE) using the Bosch process (STS Limited) with a silicon wafer as substrate was found to be the most suitable method. The resulting trenches are etched 100 μm deep with nearly vertical sidewalls. Importantly, a hydrophobic coating on the chip surface helps to confine the ink inside the channels. The channels (bottom and sidewalls) are not coated and have good wetting characteristics for hydrophilic inks, including water-based solutions of organic materials.

2.4. Application

Because of the risk of premature evaporation for certain inks, it is advisable to first align the probe array to the microwell array before adding the liquid. All following alignment and inking steps were carried out with an NSCRIPTOR instrument [5]. On this instrument, the inkwell chip is held on the same sample puck as the writing substrate, allowing for quick translation between the two surfaces. Figure 5(a) shows an array of identical, closely spaced silicon nitride probes, leveled to the inkwell surface and rotationally aligned to the microwell array. After this step, the sample puck containing both inkwell and sample is removed and a syringe with a micro-needle (Hamilton Company), mounted on a 3D micropositioner, is used to fill the reservoirs with nanoliter volume droplets. Re-inserting the sample puck and minor rotational fine-adjustment results in essentially the same video image as recorded before (figure 5(a)). Using the NSCRIPTOR software InkCAD, microwells are assigned to a captured video image and the pens are moved above the microwells and lowered until the tips make contact with the liquid in the microchannel. At this point, the cantilevers are drawn towards the surface due to capillary force and deflected. The resulting colour change in the video image can be observed in figure 5(b).

It is important to note that no ink spillage occurs during the dipping operation (see figure 5(b)) if the wetting properties of the various surfaces are selected correctly, as mentioned above. In contrast, when the inkwell chip surface is chosen to be hydrophilic and hydrophilic inks are used, the ink sometimes spills out of the channel, wets the surface and spreads from cantilever to cantilever, producing cross-contamination. Figure 6(a) shows an SEM image of one pen (lighter structure on top) in contact with the inkwell (bottom). The various devices are engineered such that the writing tip can immerse into the ink while the cantilever is prohibited from completely submerging into the channel.

Evaporative losses are the time-limiting factor for using many ink systems in inkwells. A water-based ink will remain usable for at least 10 min in ambient conditions before evaporation depletes the inkwells. Although this is already enough time to complete the inking procedure, it is possible to further increase time to dry-out by using additives such as Betaine or by simply increasing the humidity, which can be done using the environmental control chamber that is part of the NSCRIPTOR. Some macroscopic inks consist of a solvent and the chemical that, often in solid form, is used as the DPN ink once it is deposited on the tip. In these cases, the solvent is chosen to evaporate quickly once the tip is inked. We found that organic-based inks with a boiling point above 100 °C result

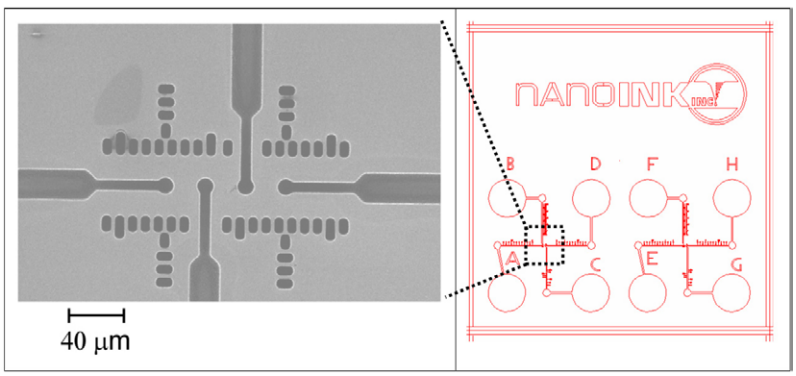

Figure 4. On the right side, one of the inkwell designs can be seen. The left side shows an SEM micrograph of the central area where four microwells with different inks are available to ink adjacent pens in a multi-probe array.

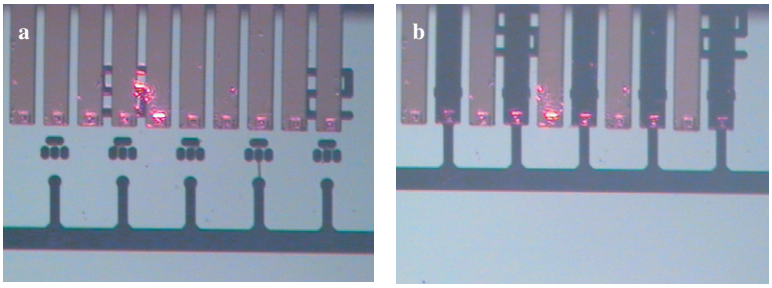

Figure 5. (a) Video image of a probe array, leveled and rotationally aligned with filled microwell array below. (b) Video image of the same setup during the inking process. Here, cantilevers that are positioned on top of microwells are deflected towards the liquid filled microwells. This changes the apparent brightness since light reflects off-axis.

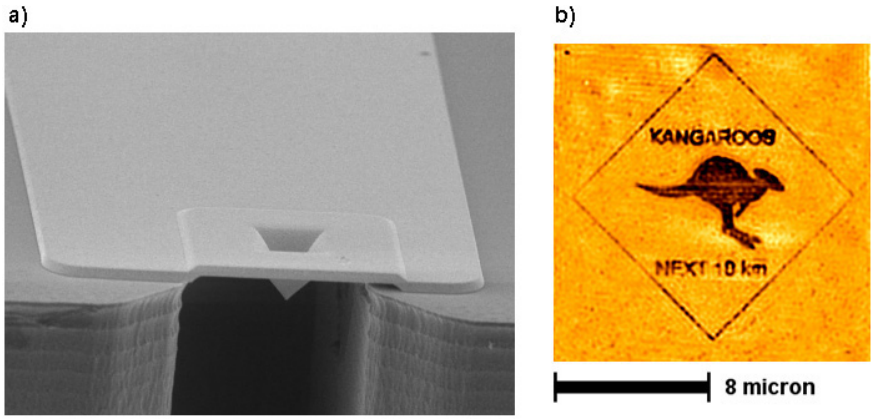

Figure 6. (a) An SEM micrograph of a pen, consisting of cantilever and tip, reaching into a microchannel. (b) A pattern written with probes inked in inkwells displays good writing quality.

in evaporation times between 30 min and 6 h in the inkwell. Inkwell inked pens showed successful writing using alcohol-based inks as well as MHA in a solvent. As an example, figure 6(b) shows a miniature kangaroo warning sign written using MHA on gold. Pens inked in inkwells show nearly the same ink diffusion coefficient as manually coated probes. As this image shows, they produce high-resolution patterns without any additional preparation steps.

3. Active probes

3.1. Motivation

The next advance in DPN technology, after adding the capability of using multiple parallel pens and the use of various different inks in parallel, is the move from arrays of passive probes to individually actuated pens. Passive probe arrays are limited to writing the same structure with all pens. This increases throughput n-fold with n pens if the desired final pattern is a repetition of the same substructure, spaced from each other by the probe pitch. For more complex and large-scale patterns, active pens are the enabling technology to use: if the actuated probes are spaced apart as far as the scanner area is across, the patterning area is effectively increased by a factor of n. If they are closer together, they have an overlapping area where multiple inks can be overlaid into a single writing space (i.e. the scanner range). In general active probe arrays can be used to produce arbitrarily complex patterns of multiple inks over large areas. In particular, complex patterns can be drawn with a succession of single adjacent linear paths. In this raster write approach the complexity of the pattern rests in the programming and timing of pen actuation rather than the complicated movement of a single pen or a passive multi-probe array.

Various actuation principles were explored, most notably thermal actuation and electrostatic actuation which have both been thoroughly investigated in the research group of Chang Liu at UIUC [22–24]. The chosen design is based on this research featuring thermal bimorph probe actuation for its simplicity in fabrication, reliability and well-documented performance. Notably, our design differs from the Liu design in that we have opposite actuation direction. This means that heating the cantilever results in bending towards the substrate. This is particularly useful if the duty cycle of each single pen is expected to be less than 50%. Furthermore, the ink is heated when writing and this allows for faster ink diffusion and thus higher writing speed. Three different heater geometries were investigated based on previously designed passive diving board probes (see figure 7).

3.2. Fabrication

Thermally actuated probes for DPN have previously been fabricated utilizing silicon nitride cantilevers with microcast

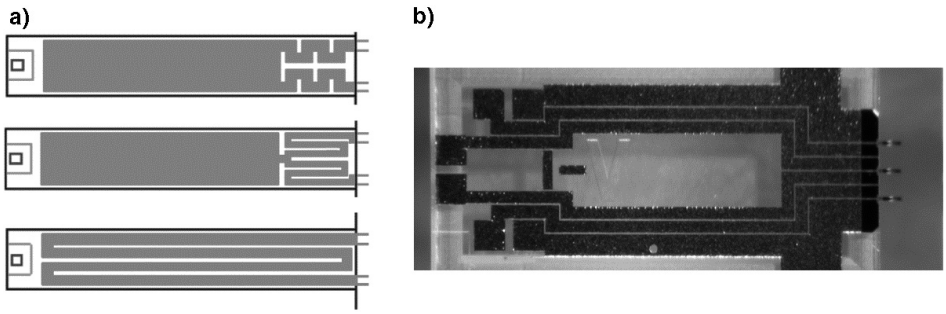

Figure 7. (a) Three different thermal bimorph topologies were fabricated. From top to bottom: 'two-lead', 'one-lead' and 'through-the-cantilever' design. (b) Video image of active pen die. The cantilevers can be seen to the right.

tips [18, 19]. These tips were formed using convex silicon molds. By using etch pits to define microcast tips we were able to realize pens that are substantially sharper, at the expense of introducing an additional bonding step. These active pens were fabricated using a modification of the design for silicon nitride AFM probes described by Albrecht *et al* [25].

After oxidizing a (100) silicon wafer, square openings are defined in the oxide. The oxide serves as a mask during a short etch of the exposed silicon in a KOH solution to form pyramidal pits bounded by (111) planes. These pits serve as molds for the formation of silicon nitride tips. The oxide is stripped, after which a second oxidation is performed to provide a sharpening contour to the inside of the tip molds [26]. A layer of low stress silicon nitride is now deposited on both surfaces of the wafer, lithographically patterned, and etched to define cantilevers with the aforementioned pits near their ends. All silicon nitride is then removed from the opposite side the structure. The thermal bimorph actuators are fabricated on the cantilevers from evaporated Cr/Pt/Au using lift-off. Interconnects and bond pads are similarly formed on a Pyrex wafer which serves as a final support for the cantilevers, after the bonding process. Finally the silicon is removed by etching in TMAH.

3.3. MEMS testing

Before the active probes are further integrated into the complete system, they must be characterized. The device's performance is defined by the electrical properties of the different heater designs, cross-talk between probes, repeatability of actuation, actuation stroke at different power levels, variation in stroke for identically designed probes, decrease in response for increasing actuation frequency and fatigue.

Joule heating is delivered to the cantilever bimorph via a gold thin-film resistor that has been patterned onto the cantilever. With the exception of the through-the-cantilever heater design, the resistor heater and bimorph are distinct, whereas in the former design the resistor and heater pattern act both as a heater and as a component of the bimorph. In the two designs where the heater is a separate pattern, it has been located at the base of the cantilevers concentrating the heat away from the probe tip. For the different cantilever lengths designed, i.e. 100, 150 and 200 μm, the heater area comprises 15%, 20%, and 30% of the total cantilever area and the bimorph component or 'heater spreader' comprises the remainder. Where the heater and bimorph are one and the same for the through-the-cantilever heater design, this does not apply.

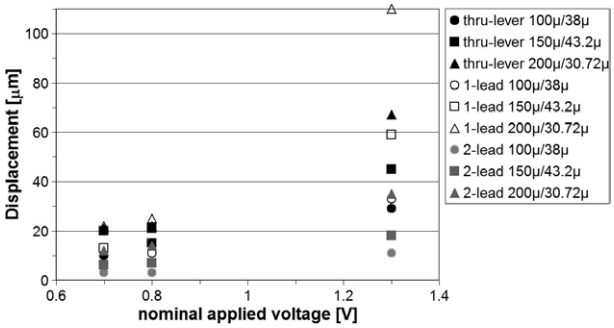

Figure 8. Measured displacement of three active cantilever designs versus nominal applied voltage. The legend shows the cantilever design, cantilever length and width.

For testing, current is delivered from a GoldStar FG-2002C function generator through probe needles to the contact pads on the Pyrex body. Resistance is measured using a Fluke 187 digital multimeter and the voltage with a Tektronix 7300 oscilloscope. (Variation in resistance among the cantilevers has been normalized.) As power is delivered, the cantilevers are actuated toward the direction normal to the heated surface—or towards the interconnect side. Displacement is determined by capturing and analyzing images of the edge displacement of the cantilever in a frontal view, using a calibrated video microscope. Figure 8 shows the results of the three different cantilever designs of various dimensions and electrical properties at different nominal voltages. Three different cantilever lengths are tested for each of the heater designs: for a length of 100 μm the cantilever width is 38 μm; for a length of 150 μm the width is 43.2 μm; and for a length of 200 μm the width is 31 μm.

For practical applications, the actuation does not need to be larger than 10 μm. A probe continuously actuated within standard operating limits performed flawlessly for the duration of the experiment, surviving 800 000 actuation cycles. For performance testing, the probes were actuated with more displacement to test reliability and to characterize the different heater designs. From the data in figure 8, it can be inferred that longer cantilevers deflect further, an expected result. The three designs behave similarly well at lower powers. At the highest power used (10 mW) the one-lead design is followed by the through-the-cantilever and two-lead design in stroke distance.

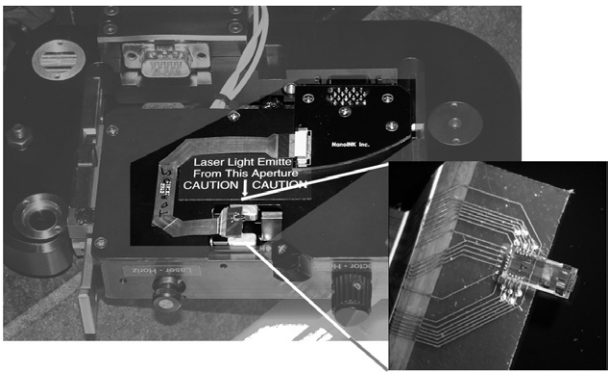

Figure 9. The larger photograph shows the NSCRIPTOR scanner from the bottom side. The high contrast area contains the interface board on the right top, the flexible cable and finally the probe assembly which can also be seen in the inset.

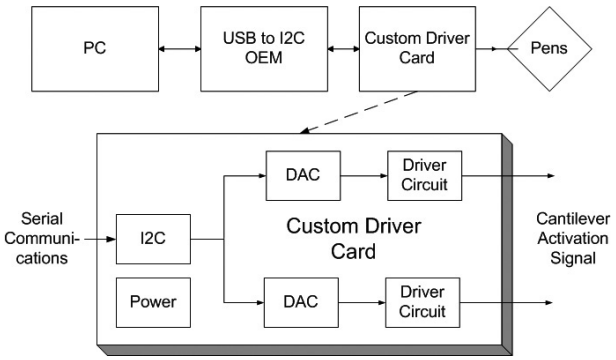

Figure 10. A block diagram showing the principal components of the active pen driving scheme on top. Below, the modular design of the custom driver card is depicted in some more detail.

Preliminary observations show that cross-talk (unwanted actuation of adjacent probes) is at or below 10% of the distance moved by the actuated probe. Upon examination of both the visible response and closer inspection of the cantilevers, we attributed this unwanted actuation to mechanical cross-talk: we observed a form of webbing or extended material overhanging along the edge between and among the cantilevers. This is a fabrication artifact that has since been solved. Cross-talk can be expected to be much lower for future fabrication runs.

3.4. Integration

The current active probe design has the same form factor as commercial passive probes, with bond pads on the far side of the die, away from the cantilevers to maximize clearance between probe assembly and sample when writing (see figure 7(b)). A successfully bonded probe can be seen in the inset of figure 9. It is wire-bonded onto a flexible circuit assembly that carries the activation signal from the driver board to the probe (see figure 9). The flex circuit was chosen for its low weight and low height which maximizes clearance to the sample.

The probe assembly is controlled by the PC through USB serial communications links. A USB-to-I2C card then generates I2C (a two wire serial communications standard) commands and passes this serial string to the custom driver card's I2C input (see figure 10). A digital-to-analog converter (DAC) receives and interprets these commands. Each output of the DAC drives the input of an analog driver stage. Utilizing the standard USB port on a PC allows for easy scaling of the system at very little cost as the system can use standard USB hubs to expand. The USB command strings are converted to the I2C bus protocol to allow the use of commercially available DACs and ADCs. The output driver signal utilizes DDS (direct digital syntheses) and therefore can take any preferred profile, i.e. the shape of the output is determined by the driver software module.

Since the probe controller solution is modularized (see figure 10), it allows for maximum flexibility. For example, a change from thermal actuation which requires moderate voltages and currents to electrostatic or piezoelectric actuation would require higher voltages than are possible with the present driver stage. The driver module can then be redesigned to meet the new requirements with a minimum impact on the rest of the system.

4. Summary and outlook

We reported on recent developments to maximize throughput and versatility of dip pen nanolithography. These developments include the design, fabrication and application of microfluidic ink delivery devices. We showed successful inking of arrays of individual writing pens and subsequent patterning using these probes. Another important development is the introduction of actuated probes. We presented the design, fabrication, integration and preliminary test results for thermally actuated pens. Active probe technology will be further optimized to work seamlessly with DPN patterning. The DPN process will be further scaled up by utilizing two-dimensional probe arrays. Such an array with over 1.3 million probes has already been built as a demonstration object and used in its most rudimentary form as a stamper. For the future, massively parallel DPN arrays with integrated and real-time ink delivery and fully actuated probes can be imagined.

Acknowledgments

This work would not have been possible without the previous and continuing DPN research and MEMS development efforts of the Mirkin research group at Northwestern University and the group of Chang Liu at the University of Illinois at Urbana-Champaign. The authors also thank all employees at NanoInk, in particular the chemistry and software team for inking applications and Joe Fragala for all matters concerning microfabrication.

References

[1] Binnig G, Rohrer H, Gerber Ch and Weibel E 1982 Tunneling through a controllable vacuum gap *Appl. Phys. Lett.* **40** 178–80

[2] Binnig G, Quate C F and Gerber C 1986 Atomic force microscope *Phys. Rev. Lett.* **56** 930–3

[3] Krämer S, Fuierer R and Gorman C 2003 Scanning probe lithography using self-assembled monolayers *Chem. Rev.* A–AZ (Review; ASAP article)

[4] Piner R, Zhu J, Xu F, Hong S and Mirkin C 1999 Dip-pen nanolithography *Science* **283** 661–3
[5] NanoInk, Inc. 1335 W. Randolph St., Chicago, IL 60607 www.nanoink.net
[6] Mirkin C A, Piner R and Hong S 2003 Methods utilizing scanning probe microscope tips and products therefor or products thereby *US Patent Specification* 6635311
[7] Fu L, Liu X, Zhang Y, Dravid V and Mirkin C A 2003 Nanopatterning of 'hard' magnetic nanostructures via dip-pen nanolithography and a sol-based ink *Nano Lett.* **3** 757–60
[8] Su M, Li S and Dravid V 2003 Miniaturized chemical multiplexed sensor array *J. Am. Chem. Soc.* **125** 9930–1
[9] Hong S H and Mirkin C A 2000 A nanoplotter with both parallel and serial writing capabilities *Science* **288** 1808–11
[10] Demers L M, Ginger D S, Park S-J, Li Z, Chung S-W and Mirkin C A 2002 Direct patterning of modified oligonucleotides on metals and insulators by dip-pen nanolithography *Science* **296** 1836–8
[11] Hong S, Zhu J and Mirkin C A 1999 Multiple ink nanolithography: toward a multiple-pen nano-plotter *Science* **286** 523–5
[12] Barone A D, Beecher J E, Bury P A, Chen C, Doede T, Fidanza J A and McGall G H 2001 Photolithographic synthesis of high-density oligonucleotide probe arrays *Nucleosides, Nucleotides Nucleic Acids* **20** 525–31
[13] Lee K-B, Lim J-H and Mirkin C A 2003 Protein nanostructures formed via dip pen nanolithography *J. Am. Chem. Soc.* **125** 5588
[14] Lee K-B, Park S-J, Mirkin C, Smith J and Mrksich M 2002 Protein nanoarrays generated by dip-pen nanolithography *Science* **295** 1702–5
[15] Zhang H, Chung S-W and Mirkin C A 2003 Fabrication of sub-50-nm solid-state nanostructures on the basis of dip-pen nanolithography *Nano Lett.* **3** 43
[16] Liu X, Fu L, Hong S, Dravid V P and Mirkin C A 2002 Arrays of magnetic nanoparticles patterned via 'dip-pen' nanolithography *Adv. Mater.* **14** 231
[17] Demers L M and Mirkin C A 2001 Combinatorial templates generated by dip-pen nanolithography for the formation of two-dimensional particle arrays *Angew. Chem. Int. Edn Engl.* **40** 3069–71
[18] Zhang M, Bullen D, Chung S-W, Hong S, Ryu K, Fan Z, Mirkin C A and Liu C 2002 A MEMS nanoplotter with high-density parallel dip-pen nanolithography probe arrays *Nanotechnology* **13** 212–7
[19] Bullen D, Chung S, Wang X, Zou J, Liu C and Mirkin C 2002 Development of parallel dip pen nanolithography probe arrays for high throughput nanolithography *Mater. Res. Soc. Proc.* **758** LL4.2.1–10
[20] Bullen D, Wang X, Zou J, Hong S, Chung S-W, Ryu K, Fan Z, Mirkin C and Liu C 2003 Micromachined arrayed dip pen nanolithography probes for sub-100 nm direct chemistry patterning *Proc. IEEE 16th Annual Int. Conf. on Micro Electro Mechanical Systems* p 4
[21] Banerjee D, Fragala J, Duenas T, Shile R and Rosner B 2003 Planar capillary pumped ink delivery apparatus for dip pen nanolithography *Micro Total Analysis Systems; 7th Int. Conf. on Miniaturized Chemical and Biochemical Analysis Systems (Squaw Valley, CA, USA, 2003)* vol 1, p 57
[22] Bullen D, Zhang M and Liu C 2002 Thermal–mechanical optimization of thermally actuated cantilever arrays *SPIE Smart Electronics, MEMS, and Nanotechnology Conf. (4700) (San Diego, CA)* pp 17–21
[23] Zhang M, Bullen D, Ryu K, Liu C, Hong S, Chung S and Mirkin C 2001 Passive and active probes for dip pen nanolithography *1st IEEE Conf. on Nanotechnology (Maui, HI)*
[24] http://galaxy.micro.uiuc.edu/research/current/nanolithography/index.html
[25] Albrecht T R, Akamine S, Carver T E and Quate C F 1990 Microfabrication of cantilever styli for the atomic force microscope *J. Vac. Sci. Technol.* A **8** 3386
[26] Akamine S and Quate C F 1992 Low temperature thermal oxidation sharpening of microcast tips *J. Vac. Sci. Technol.* B **10** 2307